Journal of Applied Polymer Science

Bio-Based Polymer Nanocomposites Based on Layered Silicates Having A Reactive and Renewable Intercalant

Özlem Albayrak,[1] Sinan Şen,[1] Gökhan Çaylı,[2] Bülend Ortaç[3]
[1]Department of Polymer Engineering, Yalova University, Yalova 77100, Turkey
[2]Department of Mechanical Engineering, Gediz University, İzmir 35665, Turkey
[3]UNAM-Institute of Materials Science and Nanotechnology, Bilkent University, Ankara 06800, Turkey
Correspondence to: S. Şen (E-mail: sinans@yalova.edu.tr).

ABSTRACT: Soybean oil-based polymer nanocomposites were synthesized from acrylated epoxidized soybean oil (AESO) combined with styrene monomer and montmorillonite (MMT) clay by using *in situ* free radical polymerization reaction. Special attention was paid to the modification of MMT clay, which was carried out by methacryl-functionalized and quaternized derivative of methyl oleate intercalant. It was synthesized from olive oil triglyceride, as a renewable intercalant. The resultant nanocomposites were characterized by X-ray diffraction (XRD) and transmission electron microscopy (TEM). The effect of increased nanofiller loading in thermal and mechanical properties of the nanocomposites was investigated by thermogravimetric analysis (TGA) and dynamic mechanical analysis (DMA). The nanocomposites exhibited improved thermal and dynamic mechanical properties compared with neat acrylated epoxidized soybean oil based polymer matrix. The desired exfoliated nanocomposite structure was achieved when the OrgMMT loading was 1 and 2 wt % whereas partially exfoliated nanocomposite was obtained in 3 wt % loading. It was found that about 400 and 500% increments in storage modulus at glass transition and rubbery regions, respectively were achieved at 2 wt % clay loading compared to neat polymer matrix while the lowest thermal degradation rate was gained by introducing 3 wt % clay loading. © 2013 Wiley Periodicals, Inc. J. Appl. Polym. Sci. 130: 2031–2041, 2013

KEYWORDS: clay; composites; mechanical properties; thermal properties

Received 4 January 2013; accepted 9 April 2013; Published online 14 May 2013
DOI: 10.1002/app.39391

INTRODUCTION

Synthetic polymers including both thermosets and thermoplastics have been widely used in the synthesis of polymer-clay nanocomposites by different methods.[1,2] However, these polymers are obtained from petroleum-based monomers and their resources are being consumed quickly and their cost increases continuously. On the other hand, polymers obtained from renewable resources have potential advantages compared with synthetic petroleum based polymers such as their low production cost and possible biodegradability.[3] To enhance properties of bio-based polymers for engineering applications, composite materials are prepared by the addition of reinforcing agents like clays and fibers to the polymer matrix.[4] Therefore, in recent years, many studies have been done to prepare polymeric composites having at least one component from renewable resources.[5–10] Among products from agricultural, natural oils contain raw materials useful in polymer synthesis. Soybean oil, which is a kind of plant oil triglyceride, is one of the most commonly used renewable resources. It mainly involves triglycerides of oleic and linoleic acids.[11] Triglyceride molecules are converted to those having polymerizable groups by using the reactive sites on them such as double bond, allylic carbon and ester groups. It is known that plant oil triglyceride based polymers do not exhibit sufficient rigidity and strength required for structural applications by themselves. In the literature, polymers with improved physical and mechanical properties have been synthesized by reacting renewable monomers with petroleum based monomers such as styrene[12–15] and diglycidyl ether of bisphenol F.[16] There are quite limited studies about the polymer nanocomposites based on the use of bio-based monomers. They have been prepared in presence of synthetic alkyl ammonium salts as intercalants.[17–20] Wool and coworkers[12] prepared the bio-based nanocomposites of functionalized plant oils and quaternary alkyl ammonium modified MMT clay by in situ polymerization. They reported that the nanocomposites resulted in a mix of intercalated and partially exfoliated structures with a 30% increase in flexural modulus. Uyama et al.[17] dispersed quaternary alkyl ammonium modified MMT clays in epoxidized soybean oil and epoxidized linseed oil by an acid catalyzed curing reaction. They obtained both intercalated and exfoliated nanocomposite structures with enhanced thermal and mechanical properties. In

all the abovementioned works, MMT clay was modified with conventional quaternary alkyl ammonium ions.

In the literature, in addition to conventional alky ammonium ions, there are also those containing styryl groups and vinyl groups used for the modification of layered clay (MMT) in polymeric nanocomposites because they participate in the polymerization reaction.[21–25]

On the other hand, a quaternized acrylated epoxidized soybean oil (AESO) derivative was used as the first renewable intercalant for the modification of the MMT clay[15] in the synthesis of AESO-based nanocomposite. It was found that the resultant nanocomposites had exfoliated nanocomposite structures with improved thermal and mechanical properties.

Recently, our group has reported the synthesis of a new renewable methyl oleate based intercalant having allylic functional group used for the modification of MMT clay in preparation of AESO-MMT nanocomposites.[26] It was synthesized from olive oil triglyceride by following three transformations which were transesterification, allylic bromination, and quaternization reactions, respectively. The three step synthesis of this intercalant was thought to be more advantageous than five steps synthesis procedure of quaternized functionalized acrylated epoxidized soybean oil based intercalant.[15] It was found that the desired exfoliated nanocomposite structure was achieved when the OrgMMT loading was 1 and 2 wt %, whereas a partially exfoliated or intercalated nanocomposite was obtained for 3 wt % loading. All the nanocomposites exhibited improved thermal and mechanical properties as compared with virgin acrylated epoxidized soybean-oil-based polymer matrix. The property enhancement observed for the nanocomposites was ascribed to a maximized interaction between the clay and the polymer matrix due to the probable contribution of the allylic group of the modifier in the polymerization reaction. However, since the allylic radical of the intercalant is too stable to reinitiate polymerization, the intercalant was expected to bind to the polymer by undergoing mostly termination reaction with reactive propagating radicals of the matrix.

This study involves a new design of biosource-based intercalant for the modification of MMT clay. The use of more reactive methacryl derivative of quaternized methyl oleate as a novel biosource-based intercalant for modification of MMT clay is thought to be more effective in preparation of exfoliated AESO-based nanocomposites with much higher mechanical and thermal properties than allylic group-functionalized intercalant.[26] In this article, we report the synthesis of a new renewable and reactive methyl oleate based intercalant, quaternized methyl oleate, for the modification of MMT clay and its use in preparation of bio-based polymer nanocomposites. Quaternized and reactive methyl oleate was synthesized from olive oil triglyceride by following three transformations which were transesterification, allylic bromination and quaternization reaction with *N,N*-(dimethylamino) ethyl methacrylate, respectively. Acrylated epoxidized soybean oil (AESO) and styrene mixture was polymerized by *in-situ* free radical polymerization in the presence of the quaternized and reactive methyl oleate-modified MMT clay in order to obtain polymeric nanocomposites. Unlike the allylic functionalized intercalant,[26] through the use of a reactive quaternized methyl oleate intercalant with relatively bigger and longer methacryl moiety which acts as a more effective spacer, we expected to get increased expansion of the clay galleries. Moreover, the organic modifier is expected to participate in polymerization reaction via its reactive double bond leading to enhanced mechanical strength and thermal properties as well as exfoliated nature in the nanocomposites. The effect of organoclay content on the dynamic mechanical, thermal and morphological properties of the resultant nanocomposites are discussed in detail.

EXPERIMENTAL

Materials

Acrylated epoxidized soybean oil (AESO) was obtained from Sartomer Company (Exton, PA, USA). This AESO is acrylated with approximately 3.5 acrylates per triglyceride and an average molecular weight of 1200 g/mol. *N,N*-(dimethylamino) ethyl methacrylate (DMAEM) was purchased from Aldrich (Steinheim, Germany) and used as received. Styrene (Aldrich, Steinheim, Germany) was used without any purification. The clay, sodium montmorillonite (NaMMT) was kindly donated by Süd Chemie, (Moosburg, Germany) (Nanofil 1080; cationic (Na^+) exchange capacity of 100 meq/100 g). 2,2′-Azoisobutyronitrile (AIBN) was obtained from Merck (Darmstadt, Germany) and dried in vacuum at room temperature. Olive oil was supplied by Komili (İstanbul, Turkey). Syntheses of methyl oleate and allylic brominated methyl oleate were carried out in a similar manner to that reported previously.[27–30]

Synthesis of Methacryl-Functionalized Quaternary Ammonium Salt of the Allylic Brominated Methyl Oleate

Ten grams of allylic brominated methyl oleate (ABMO) (0.0266 mol) was diluted in 20 mL of THF. Four grams of *N,N*-dimethylamino ethyl methacrylate (DMAEM) (0.0266 mol) was added into this solution. After 1 h, the solution became turbid. Then, the solution was stirred overnight at 50°C under N_2 atmosphere. Then, THF was evaporated in a rotary evaporator and the crude product (QMO) was used without any purification. Figure 1 shows the quaternization reaction of ABMO.

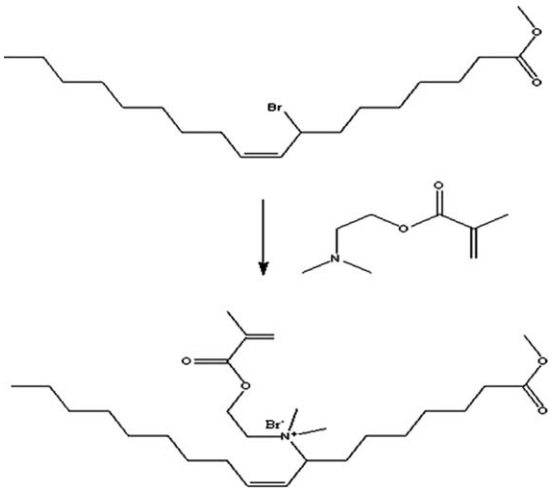

Figure 1. Quaternization of ABMO.

Modification of NaMMT Clay with the Quaternized Methyl Oleate

NaMMT (2 g) was dispersed in a 300 mL solvent mixture of THF and deionized water in equal volumes at 50°C. A separate solution of 2 g quaternized methyl oleate (QMO) in the same amount of solvent mixture and composition was slowly added to the clay solution and mixed vigorously, while keeping the temperature of the solution at 50°C for 4 h. The organically modified MMT (OrgMMT) was recovered by filtering the solution, followed by repeated washings of the filter cake with THF-deionized water mixture to remove any excess ions. The final product was dried at 50°C in a vacuum oven for 48 h.

Preparation of Nanocomposites

The modified clay, OrgMMT (1, 2, or 3 wt %, with respect to the monomer) was mixed with the monomer mixture which has 50 wt % AESO and 50 wt % styrene, under a nitrogen atmosphere at 50°C for 5 h. The AIBN initiator (1 wt %, with respect to the monomer) was then added to the monomer-clay solution and stirred. Then, the polymerization reaction was carried out at 50°C for 24 h and post-cured at 110°C for 2 h to obtain AESOPS nanocomposites, namely AESOPS1M-C, AESOPS2M-C, and AESOPS3M-C.

Characterization

^{1}H-NMR spectra were recorded on a 400 MHz Varian Mercury-VX NMR spectrometer (Varian Associates, Palo Alta, CA). Fourier-transform infrared (FTIR) spectra of samples were obtained with a Perkin Elmer 1600 FTIR spectrophotometer (Massachusetts, USA).

In order to measure the basal spacing (d_{001} reflection) of MMT clays, wide angle X-ray diffraction (XRD) measurements were conducted on a Rigaku D/Max-Ultimate diffractometer (Rigaku, Tokyo, Japan) with CuK$_\alpha$ radiation (λ = 1.54°A), operating at 40 kV and 40 mA and a scanning rate of 0.2 deg/min.

Morphology of the nanocomposites was investigated by both XRD and transmission electron microscopy (TEM) measurements. TEM analysis was performed using a FEI TecnaiTM G2 F30 (FEI, Hillsboro, OR) instrument operating at an acceleration voltage of 200 kV. About 100 nm ultrathin TEM specimens were cut by using cryo-ultramicrotome (Leica EMUC6/EMFC6, Vienna, Austria) equipped with a diamond knife. The ultrathin samples were placed on copper grids for TEM analyses.

The fracture surfaces of the composites were investigated by scanning electron microscopy (SEM) analysis, using ESEM-FEG and EDAX Philips XL-30 microscope (Philips, Eindhoven, The Netherlands).

Thermogravimetric analysis (TGA) was performed on a Seiko TG/DTA 6300 thermal analysis system instrument (Seiko Instruments Inc., Tokyo, Japan) under nitrogen flow with a heating rate of 10°C/min. Dynamic mechanical properties of the composites were measured with a dynamic mechanical analyzer (DMA Q800, TA Instruments, New Castle, DE) in single cantilever mode at a frequency of 1 Hz and at a heating rate of 3°C/min. The average dimensions (w x l x t) of the molded samples were 12 × 30 × 2.5 mm^3.

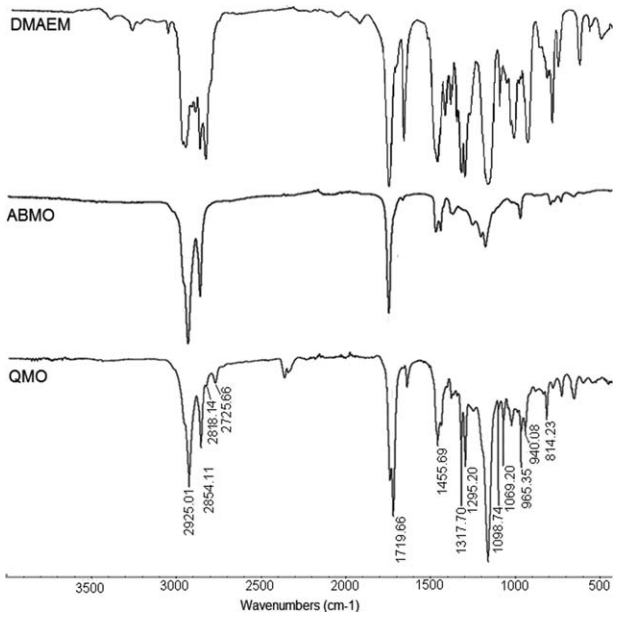

Figure 2. FTIR spectra of DMAEM, ABMO, and QMO.

RESULTS AND DISCUSSION

Synthesis of Quaternized Methyl Oleate Intercalant

Characterization of the quaternary ammonium salt of methyl oleate (QMO) was done by IR (Figure 2) and ^{1}H-NMR (Figure 3) techniques. IR spectra (Figure 2) showed the same characteristic peaks for both ABMO and QMO. The peak observed at around 2750 cm^{-1} was probably due to the C-H stretching of the dimethyl ammonium group. The peaks appeared at 1640 cm^{-1} belong to double bonds. The peaks of fatty acid methyl ester and acrylate ester groups are depicted at 1740 and 1719 cm^{-1}

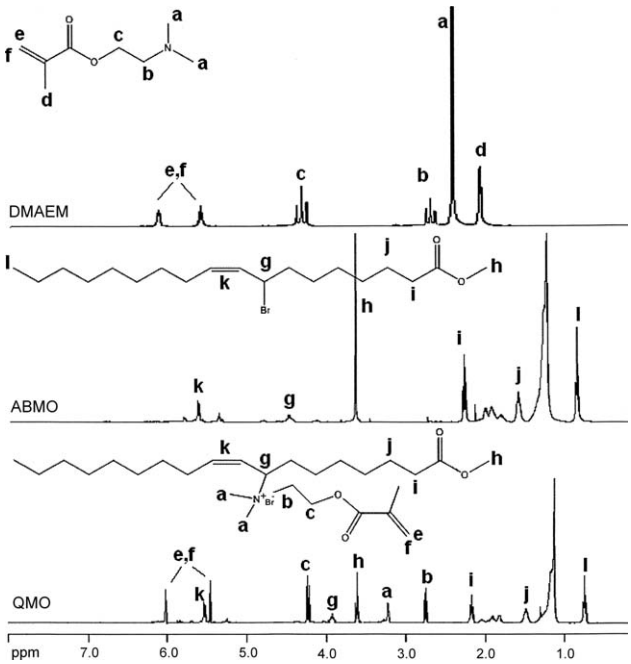

Figure 3. ^{1}H-NMR spectra of ABMO and QMO.

Table I. XRD Data for Clays and Nanocomposites

Material	d_{001} of clay, Å[a]
NaMMT	12.13 (7.28°)
OrgMMT	35.30 (2.50°)
AESOPS1M-C	No reflection
AESOPS2M-C	No reflection
AESOPS3M-C	29.25 (3.01°)

[a] Two-Theta angles are given in parentheses.

respectively. New C-H stretching peaks appeared at the spectrum of QMO at 2818 and 2720 cm^{-1} and they probably belong to -CH_2- groups of quaternized *N,N*-dimethyl amino ethyl methacrylate part of the salt. This observation is congruent with the literature.[31,32] Also, the peaks at 1317, 1295, 1098, 1069, and 1020 cm^{-1} were probably due to C-N out of plane bending vibration.

When quaternization occurred, a new peak was observed at 3.9 ppm which belongs to allylic hydrogens that is geminal to quaternary ammonium group. ^{1}H NMR spectrum of QMO also showed peaks that appear at 5.5 and 6.0 ppm belonging to the double bond hydrogens of methacrylate group. The peaks observed at 1.75 ppm are due to methyl hydrogens of methacrylate group. The peak appeared at 2.75 ppm belongs to α-hydrogens to quaternary ammonium salt. Peaks at 3.2 ppm are belong to the methyl hydrogens of quaternary ammonium salt. Integration of the all peaks is congruent with each other.

Modification of NaMMT Clay

Modification of the MMT clay was followed by X-ray diffraction analysis. XRD analysis gave the values of the interlayer spacing or *d*-spacing of the NaMMT and OrgMMT which were obtained from the peak position of the d_{001} reflection in the diffraction patterns (Figure 4). The XRD data are given in Table I. A 2θ angle of 7.28 ° and basal spacing of 12.13 Å was found for NaMMT clay. It can be seen from Table I and Figure 4 that the interlayer spacing of the OrgMMT clay was found to be 35.30 Å together with a decrease in the diffraction angle (2.5°). Thus, a decrease in the diffraction angle and increase in interlayer distance indicates that intercalation of this new renewable and reactive quaternized methyl oleate (QMO) into MMT clay layers through the ion-exchange reaction was successful, resulting in organophilic clay.

The existence of the metharcyl-functionalized and quaternized methyl oleate intercalant in the MMT structure was also confirmed by TGA. Figure 5 shows the TGA thermograms of NaMMT and OrgMMT clays and their derivative curves of weigh loss. It is clear from the figure that OrgMMT shows a lower decomposition onset temperature as well as higher degradation dependent weight loss compared to pure NaMMT. Pure MMT has only 7.5% total weight loss indicating water removal. After the intercalation, this amount reaches almost 40% at higher temperatures, resulting from the degradation of intercalated and edge/surface attached methyl oleate [Figure 5(a)]. As it can be seen from the first derivative curves of the weight loss [Figure 5(b)] that NaMMT was found to have two distinctive weight loss at 60 and 600°C most probably due to removal of moisture and bound water present in the clay galleries, respectively. On the other hand, TGA trace of the OrgMMT was completely different. It showed maximum weight loss at temperatures, 200, 300, and 360°C with much higher weight loss compared to NaMMT clay. This result can be accepted as an indication of the successful modification of the MMT clay.

Structural Morphology of the Nanocomposites

XRD analysis was used to identify the polymer nanocomposite structures as exfoliated or intercalated. Figure 6 shows the XRD

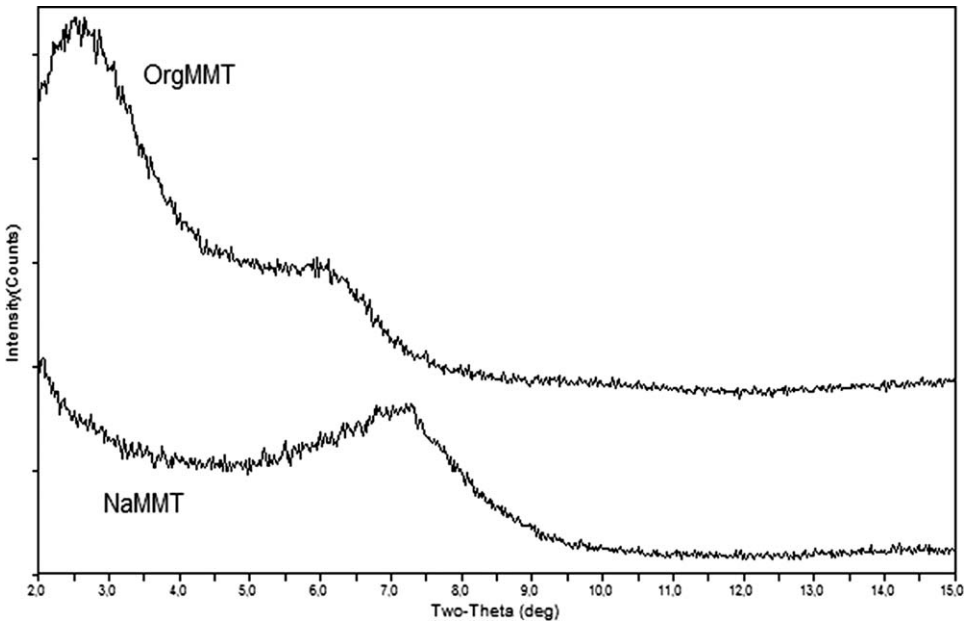

Figure 4. XRD patterns of NaMMT clay and organoclay.

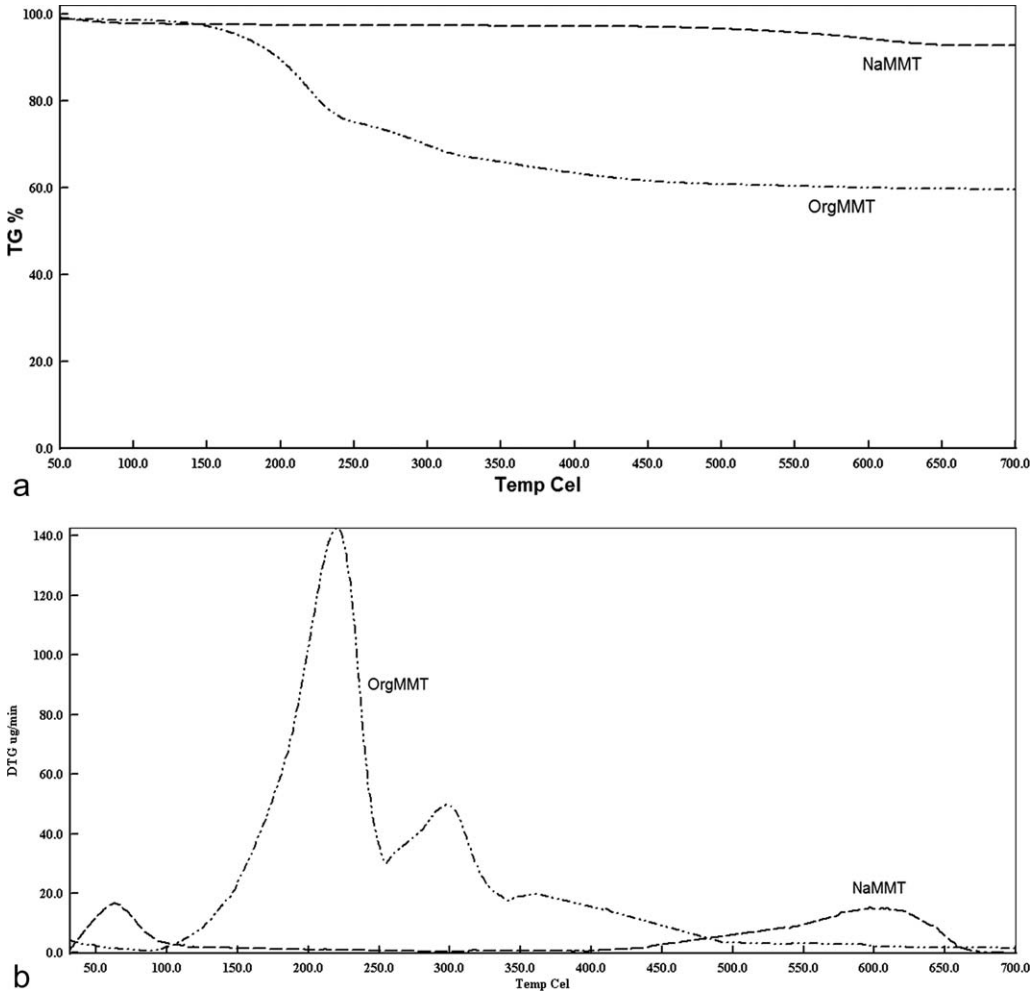

Figure 5. (a) TGA thermograms of NaMMT clay and organoclay and (b) derivatve curves of weight loss.

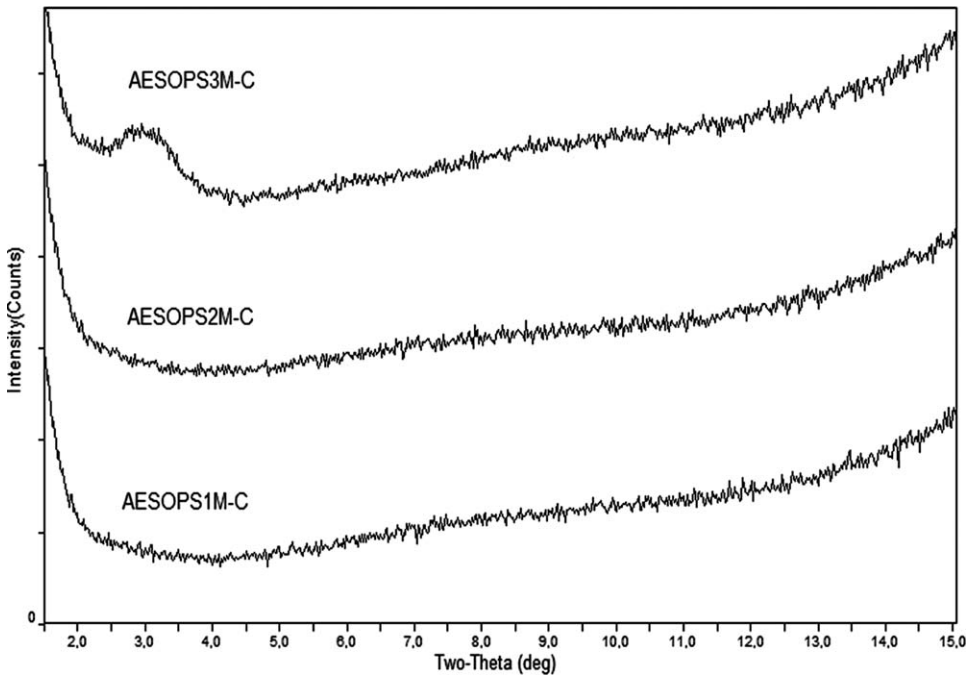

Figure 6. X-ray diffraction curves of AESOPS nanocomposites.

Applied Polymer SCIENCE

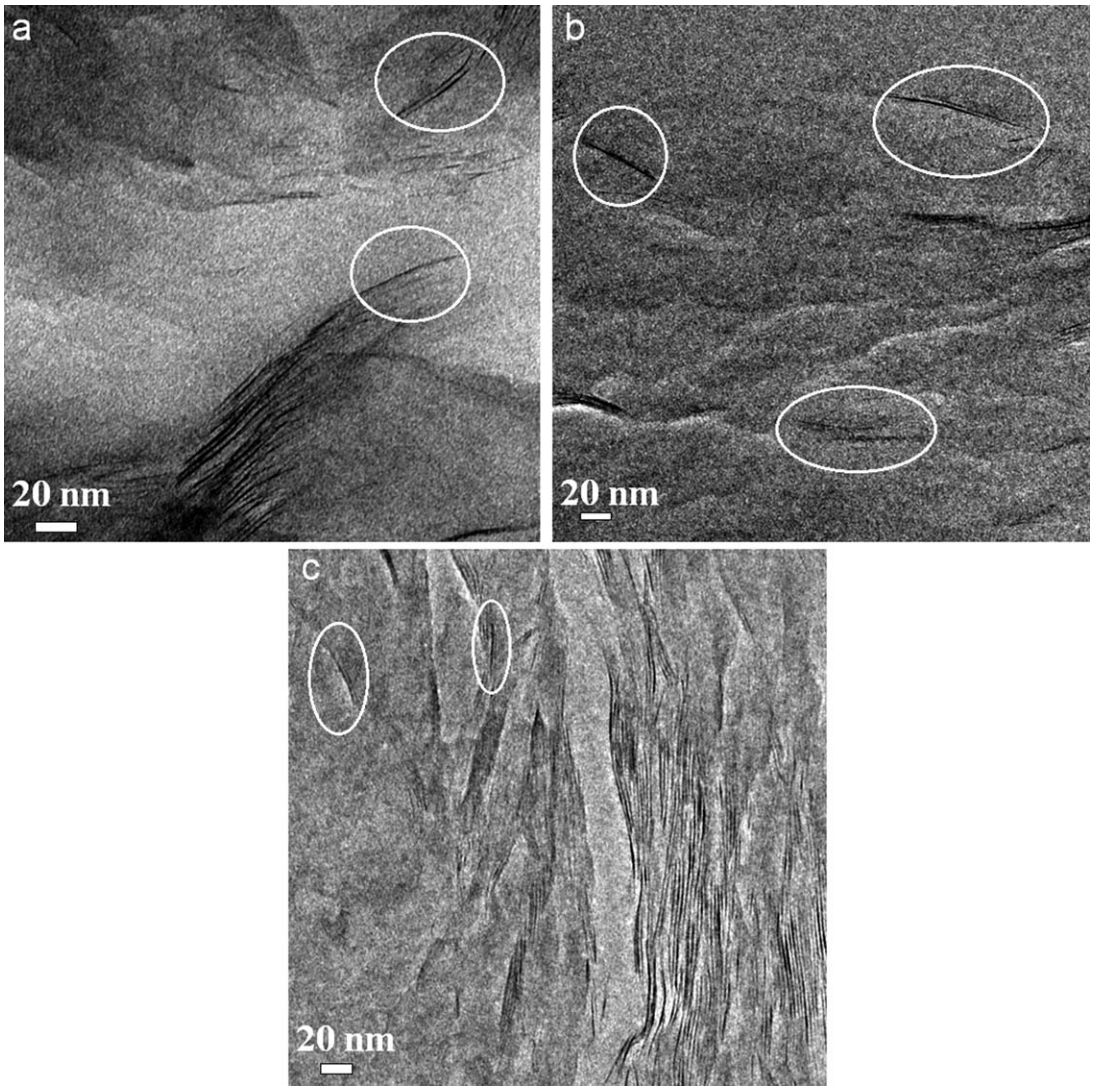

Figure 7. Low-magnification TEM images of AESOPSM-C nanocomposites; (a) AESOPS1M-C, (b) AESOPS2M-C, and (c) AESOPS3M-C (scale bar: 20 nm).

curves of the AESOPSM-C nanocomposites that were obtained by dispersing the organically modified clay in 1, 2, and 3 wt % loading in the monomer mixture of AESO and styrene. The XRD data are also summarized in Table I. It can be seen that the nanocomposites, AESOPS1M-C and AESOPS2M-C did not exhibit any d_{001} reflection in the XRD region either because of a much too large spacing between the layers or because the nanocomposite does not present ordering any more resulting in an exfoliated nature.[1] This may be possibly due to good swelling of OrgMMT clay in 1 and 2 wt % loading and homogeneous and fine dispersion of it in the matrix. On the other hand, the nanocomposite, AESOPS3M-C exhibited a small and broad peak in the relevant angle region representing the diffraction from the (001) crystal surface of the silicate layers as an indication of partially intercalated nanocomposite structure. Based upon this information, it seems that there might be relatively more attractive forces between the clay layers at higher loading which may lead to some intercalated tactoids with a small peak in XRD analysis.[29]

The morphology of the nanocomposites was also investigated by TEM analysis as one of complementary techniques for XRD and the images were displayed in Figures 7 and 8 in two different magnification scales. The dark lines observed in the TEM images represent individual silicate clay layers. As it can be seen from the images, all the nanocomposites have some irregular dispersion of the silicate layers. Some particles of the silicate layers were fully exfoliated (white circles) with orientation in different directions, while some kept an ordering of the expanded layers. Exfoliation is quite clear for AESOPS1M-C nanocomposite and the nano-sized clay layers with an average thickness of 1 nm are separated from each other in a broad range of separation (44–77 Å). For the nanocomposite AESOPS2M-C, exfoliated OrgMMT silicate layers with a thickness of layered silicate of 1 nm and in a broad range of separation (50–70 Å) can also be seen in the Figures 7 and 8. Even though the AESOPS1M-C and AESOPS2M-C nanocomposites showed no peak in its XRD pattern (Figure 6), the TEM analysis resulted in a partially exfoliated structure with relatively more exfoliated silicate layers and a few laminated silicate layers

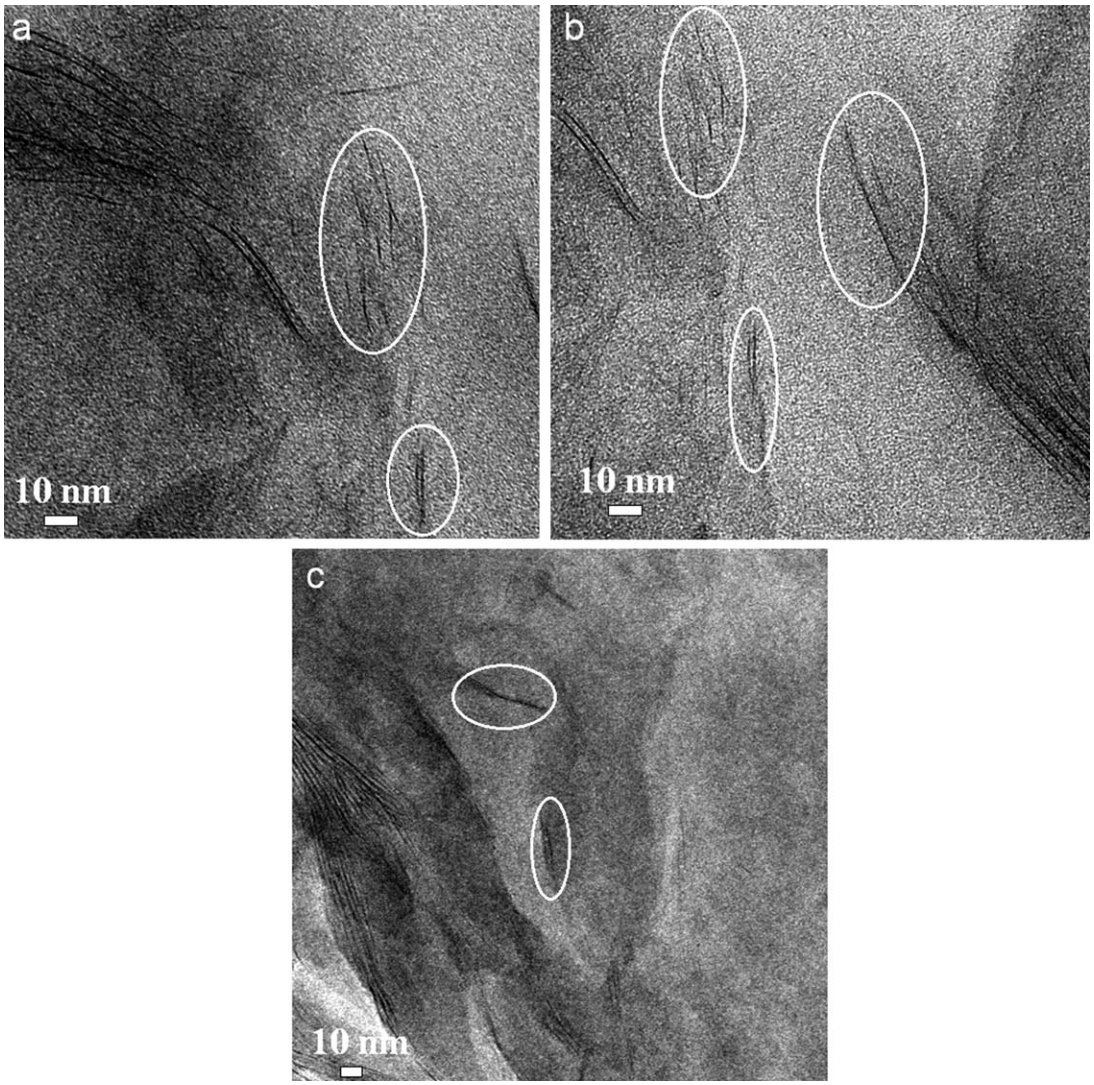

Figure 8. High-magnification TEM images of AESOPSM-C nanocomposites; (a) AESOPS1M-C, (b) AESOPS2M-C, and (c) AESOPS3M-C (scale bar: 10 nm).

in comparison with other nanocomposite, AESOPS3M-C. Disappearance of XRD peak and presence of relatively high amount of exfoliated layered silicates in AESOPS1M-C and AESOPS2M-C may be explained by homogeneous and fine dispersion of clay layers in the polymer matrix at 1 and 2% clay loading.

In the case of AESOPS3M-C nanocomposite [Figures 7(c) and 8(c)], one can easily see intercalated nanocomposite structure together with some exfoliated OrgMMT layers with a thickness of 1 nm (white circles). For this nanocomposite, the separation between the dispersed platelets is also irregular and in the broad range of 24.5–78 Å which is in good agreement with its XRD result (Figure 6). Based on this information, one can postulate that the nanocomposite AESOPS3M-C may also have a partially intercalated structure.[1]

Thermal and Mechanical Properties of AESOPSM-C Nanocomposites

The thermal stabilities of neat AESOPS matrix and the nanocomposites were studied by thermogravimetric analysis (TGA) and shown in Figures 9 and 10. The onset degradation temperature at which 5% degradation occurs (Td_5), representative of the onset temperature of degradation and the mid-point degradation temperatures (Td_{50}) together with char yield are all given in Table II.

As it can be seen from the TGA trace (Figure 9) and Table II, although the differences in thermograms seem to be small, all the nanocomposites degrade at a slightly faster rate in the temperature range of 180–400°C compared with pure polymer. For the nanocomposites, the weight loss in the abovementioned temperature range is most probably resulted from degradation of intercalant as well as water on clay surface and that between silicate layers. These nanocomposites display retardation of the thermal degradation above 425°C. On the other hand, it is clear from the figure and Table II, char yield of all the nanocomposites was found to be higher than that of neat AESOPS and increase with increasing OrgMMT clay loading. The midpoint degradation temperatures (Td_{50}) of the nanocomposites were found to be very close to that of neat UPE (Table II).

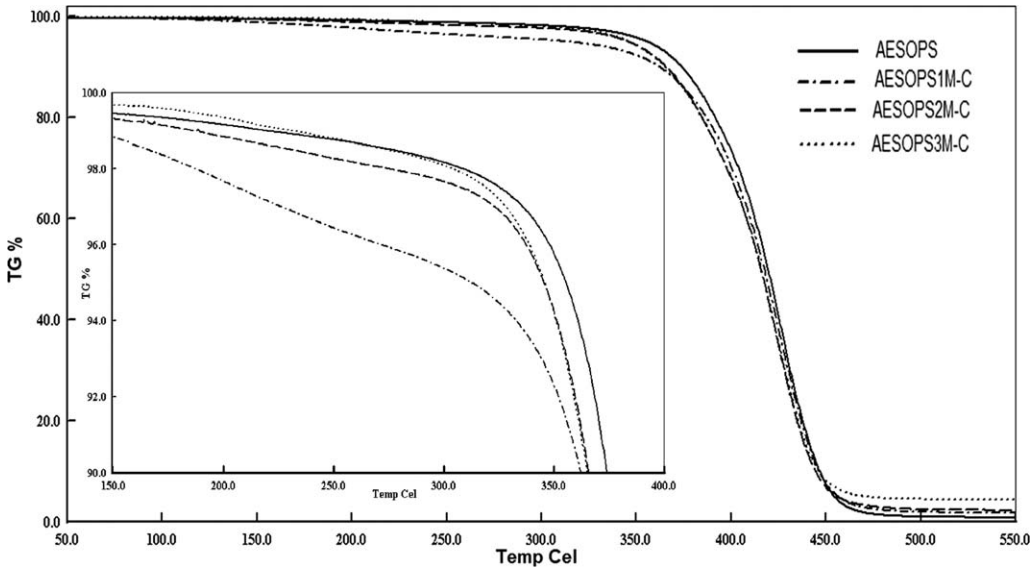

Figure 9. TGA thermograms of neat AESOPS matrix and its nanocomposites.

The peak maximum temperature values from the first derivative (DTG) of weight loss (Figure 10), which is representative of the temperature at which maximum rate of weight loss occurs, are also given in Table II. Although, the maximum temperatures of the derivative curves of the nanocomposites seems to be unchanged, all the nanocomposites exhibited a much slower degradation rate at their maximum weight loss temperature compared to neat AESOPS. The rate of decomposition at the maximum weight loss temperature was found to decrease with increasing amount of OrgMMT. This result may be attributed to the promotion of polymerization from inside the clay galleries and also from surface/edges of the clay with the help of methacryl reactive double bond present in the intercalant, bonded to the clay which leads to decrease in degradation rate of the polymer around clay surface in the nanocomposites. On the other hand, the lowest degradation rate of the AESOPS3M-C may be attributed to the confinement of AESOPS matrix between the MMT layers in alternating multilayered structure of polymer and the clay in the intercalated system.[30,33] The more compact silicate-matrix in multilayered intercalated systems (Figures 6 and 7) may cause a decrease in permeability or diffusivity of volatile degradation products. In other words, it may cause hindered out-diffusion of the volatile decomposition products or at least slow down escape of them from interlayer galleries.[34] Therefore, it can be safely stated that AESOPS3M-C nanocomposite, with the lowest degradation rate and, the modest degradation onset temperature and midpoint degradation temperature, as well as the highest char yield, has the highest thermal stability relative to other nanocomposites and neat matrix. Moreover, in comparison with AESOPS matrix, the enhanced thermal stability of the nanocomposites may be attributed to extensive interaction of polymer chains with nanodispersed OrgMMT clay, so leading to restricted

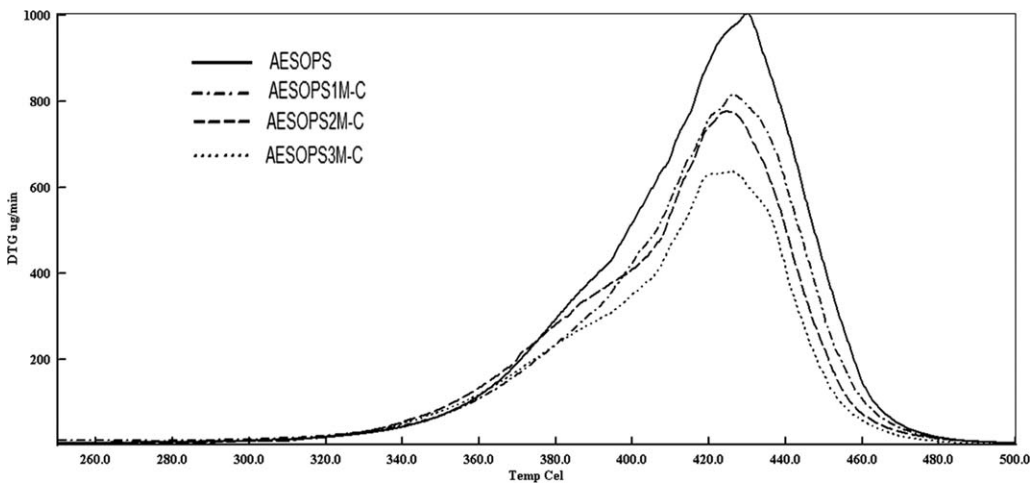

Figure 10. TGA derivative thermograms of neat AESOPS matrix and its nanocomposites.

Table II. TGA Data for Neat AESOPS and AESOPS Nanocomposites

Material	Td_5 (°C)[a]	Td_{50} (°C)[a]	Maximum rate of weight loss[b] (μg/min at °C)	Char content at 500°C (%)[a]
AESOPS	373.80 (6.71)	419.50 (3.58)	1004.00 (2.93) at 430.00 (2.34) °C	0.99 (0.31)
AESOPS1M-C	362.20 (3.13)	417.50 (4.04)	814.80 (4.91) at 426.00 (4.02) °C	1.98 (0.12)
AESOPS2M-C	365.80 (3.22)	415.80 (2.18)	775.50 (4.83) at 424.70 (4.42) °C	2.44 (0.13)
AESOPS3M-C	365.00 (2.36)	416.00 (2.04)	635.70 (1.31) at 426.10 (0.93) °C	4.50 (0.16)

[a] Calculated from weight loss versus temperature curve of TGA thermograms.

[b] Calculated from derivative thermograms.

Data in parentheses represent standard deviations.

molecular mobility of the polymer chains and resulting in inhibition of the diffusion of the decomposed product in the polymer matrix.[35]

The dynamic mechanical performances of AESOPS and its nanocomposites were investigated by dynamic mechanical analysis (DMA). Two different parameters were determined as a function of temperature. The tan delta versus temperature and storage modulus (E') versus temperature plots are all shown in Figures 11 and 12, respectively. The glass-transition temperature (T_g) was taken as the maximum tan delta peak point which was calculated from the E'' (loss modulus)/E' (storage modulus) ratio.[34–36] The shift of the tan delta peak to higher temperatures indicate an increase in the glass-transition temperature (T_g) and enhanced thermo mechanical properties.

Compared with neat AESOPS, all the nanocomposites were found to have higher tan delta peak temperatures or T_g values. The nanocomposites, AESOPS2M-C and AESOPS3M-C display much higher increase in the tan δ peak temperature (Figure 11), which is also in good agreement with higher increase in the storage modulus compared to AESOPS1M-C (Figure 12). This may be probably due to higher contribution of reactive methacryl part and allylic part of the modifier in the polymerization at higher clay loadings, leading to a strong interaction between clay layers and polymer matrix.

The storage moduli at 50°C and 70°C were determined and reported in Table III. It is well known that whether in static or dynamic tests, the modulus change under T_g is not very clear and sensitive because of the highly restricted motion of the chains with very low energies. In Figure 12, as a much more meaningful comparison, the moduli of all the nanocomposites around T_g (50°C) and above T_g (70°C), were observed to be higher than that of the neat AESOPS (Table III) which is consistent with lower the maximum tan delta peak values (Figure 11). This might be ascribed to a maximized interaction between the clay and the polymer matrix most probably due to above-mentioned contribution of reactive methacryl and allylic groups of the modifier in the polymerization process.[37,38] It can be clearly seen from the Table III that the storage modulus of the AESOPS1M-C was found to be about 24% higher than that of neat AESOPS matrix. About 400% and 350% increase in storage modulus around T_g was achieved as a result of incorporation of 2 wt % and 3 wt % of OrgMMT clay into the AESOPS matrix, respectively. Although, in our previous study,[26] the storage modulus was found to increase about 140% for AESOPS in presence of only allylic-functionalized intercalant and at 2 wt % clay loading, having extraordinary high storage modulus for the nanocomposites in this study is remarkable.

Moreover, the rubbery plateau moduli at 70°C of the nanocomposite AESOPS2M-C and AESOPS3M-C are about six times higher than that of neat AESOPS. This is a strong advantage of

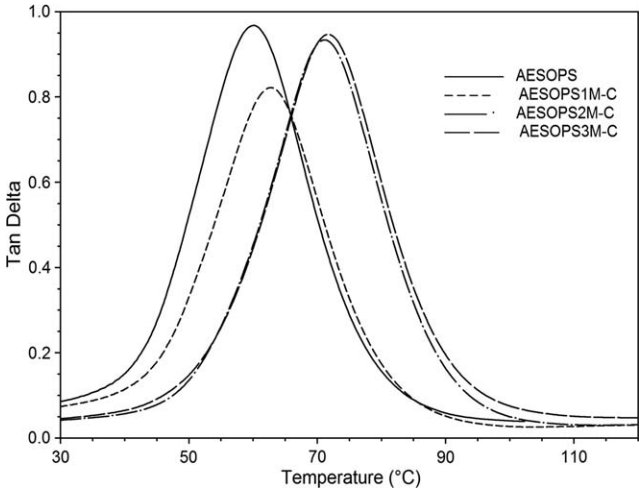

Figure 11. Tan δ versus temperature plots of neat AESOPS matrix and its nanocomposites.

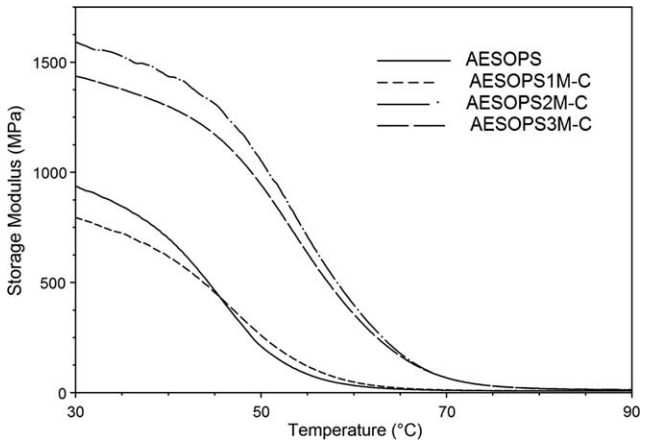

Figure 12. Storage modulus versus temperature plots of neat AESOPS matrix and its nanocomposites.

Table III. DMA Data for Neat AESOPS and AESOPS Nanocomposites

Material	E' at 50°C (MPa)	E' at 70°C (MPa)
AESOPS	210.40 (3.69)	10.68 (1.04)
AESOPS1M-C	260.10 (2.79)	12.31 (0.97)
AESOPS2M-C	1053.00 (19.95)	67.13 (3.98)
AESOPS3M-C	948.30 (12.35)	64.35 (2.99)

Data in parentheses represent standard deviations.

nanocomposite that it is able to retain a high modulus even at temperatures above the glass transition temperature. The highest value of storage modulus for AESOPS2M-C behavior can be attributed to the extraordinarily large aspect ratio of exfoliated silicate layers with good dispersion of organoclay particles in the polymer matrix (Figures 6 and 7). This increases the polymer–clay interactions, making the entire surface area available for the polymer which prevents the segmental motions of the polymer chains near organic–inorganic interfaces[39,40] and leading to dramatic changes in mechanical properties.

SEM Analyses of Fracture Surfaces of the Nanocomposites

The morphological appearance of the fracture surfaces is shown in the SEM micrographs in Figure 13. In pure AESOPS, a brittle fracture surface with cracks of large size is observed, typical of a glassy material. The image of AESOPS3M-C shows a heterogeneous fracture surface having cracks with poor distribution and different sizes as well as some areas without any crack propagation. This result may be due to incomplete dispersion of the reinforcing phase inhibiting enough surface contact between the polymer and clay, leading to large regions of pure polymer in the intercalated structure (Figure 6) of the composite. The nanocomposite AESOPS1M-C, which has a partially exfoliated nanocomposite structure (Figures 7 and 8) with absence of X-ray diffraction peak (Figure 6), indicated a better crack distribution in its fracture surface than neat AESOPS and AESOPS3M-C. The AESOPS2M-C nanocomposite exhibited a more homogeneous fracture surface with crack propagation along a more "tortuous path," which may be ascribed to much better dispersion and adhesion of the OrgMMT clay in the matrix and which is highly consistent with the XRD data without any d_{001} reflection (Figure 6) and modest damping temperature and the highest stiffness for the related nanocomposite (Figures 11 and 12).

CONCLUSIONS

Acrylated epoxidized soy bean oil (AESO)-based nanocomposites were successfully prepared by *in situ* free radical polymerization of AESO-styrene monomer mixture in the presence of montmorillonite (MMT) clay. Organically and functionally modified MMT clay was used as nanosized reinforcer in different loading degrees. Organophilic modification of NaMMT clay was carried out with a renewable intercalant, quaternized methlyl oleate (QMO) having a methacryl group making it a reactive intercalant. The effect of the renewable intercalant with double bond contribution on the properties of AESO-based polymeric nanocomposite was discussed in terms of structural, mechanical and thermal properties. Success in both intercalation

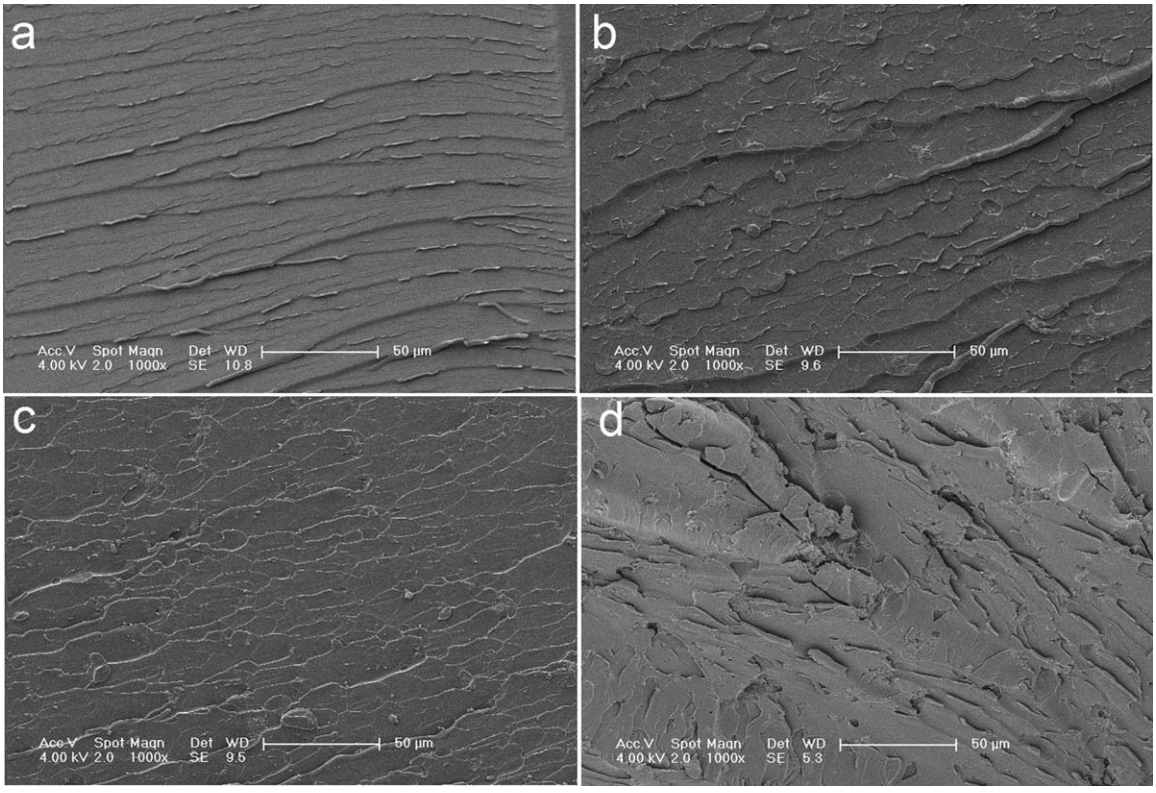

Figure 13. SEM micrographs of the fracture surfaces of (a) neat AESOPS, (b) AESOPS1M-C, (c) AESOPS2M-C, and (d) AESOPSM-C nanocomposites.

of intercalant into MMT clay layers through the ion-exchange reaction and nanosized dispersion of clay in polymer matrix were confirmed via XRD, TGA, and TEM analyses. All the nanocomposites were found to have partially exfoliated structures. AESOPS nanocomposites at 1 and 2 wt % clay loadings exhibited relatively high degree of exfoliation as evidenced by the absence of any diffraction peak in the XRD region and delamination of relatively more silicate layers as thin platelets in the matrix as observed in its TEM image. All the polymer nanocomposites were found to have higher thermal stability and better dynamic mechanical properties as compared to neat polymer matrix. This is probably due to the polymerization reaction occurring in between silicate layers and from the edge/surface of the modified clay through the intercalated and edge/surface attached reactive intercalant. The highest storage modulus increment (ca. 400%) and damping temperature was obtained for the AESOPS2M-C nanocomposite even with a clay content as low as 2 wt % which exhibited partially exfoliated nanocomposite structure having relatively higher exfoliation of the clay layers. Accordingly, SEM image of the fracture surface of the AESOPS2M-C showed that presence of OrgMMT clay with a homogeneous and nanosized dispersion in the polymer matrix, led to crack propagation along a more "rougher" path compared to AESOPS matrix. AESOPS3M-C nanocomposite with relatively high amount of intercalated nature, on the other hand, showed the best thermal stability with the lowest degradation rate and the highest char yield. As a result it can be safely concluded that partially exfoliated AESO-based nanocomposites with different degrees of exfoliation can be prepared as thermally stable and high strength by using functionally and organically modified clay with a renewable intercalant in 1–3 wt % clay loadings.

ACKNOWLEDGMENTS

Supports given by Yalova University Scientific Research Projects Coordination Department (Projects no. 2012-037) are gratefully acknowledged.

REFERENCES

1. Alexandre, M.; Dubois, P. *Mater. Sci. Eng. R: Rep.* **2000**, *28*, 1.
2. Ray, S. S.; Okamoto, M. *Prog. Polym. Sci.* **2003**, *28*, 1539.
3. Kaplan, D. L. Biopolymers from Renewable Resources; Springer: New York, **1998**.
4. Liu, Z. S.; Erhan, S. Z. *Mater. Sci. Eng. A* **2008**, *708*, 483.
5. Khot, S. N.; Lascala, J. J.; Can, E.; Morye, S. S.; Williams, G. L.; Palmese, G. R.; Kusefoglu, S. H.; Wool, R. P. *J. Appl. Polym. Sci.* **2001**, *82*, 703.
6. Chang, K. H.; Wool, R. P. *J. Appl. Polym. Sci.* **2005**, *95*, 1524.
7. Williams, G. I.; Wool, R. P. *Appl. Compos. Mater.* **2000**, *7*, 421.
8. Liu, Z. S.; Erhan, S. Z.; Xu, J.; Calvert, P. D. *J. Am. Oil Chem. Soc.* **2004**, *81*, 605.
9. O'Donnell, A.; Dweib, M. A.; Wool, R. P. *Compos. Sci. Technol.* **2004**, *64*, 1135.
10. Liu, Z. S.; Erhan, S. Z. *Mater. Sci. Eng. A*, **2008**, *483*, 708.
11. Liu, K. Soybeans: Chemistry, Technology, and Utilization; Chapman & Hall: London, **1997**.
12. Lu, J.; Hong, C. K.; Wool, R. P. *J. Polym. Sci. Part B: Polym. Phys.* **2004**, *42*, 1441.
13. Hong, C. K.; Wool R. P. *J. Appl. Polym. Sci.* **2005**, *95*, 1524.
14. Lu, J.; Khot, S.; Wool R. P. *Polymer* **2005**, *46*, 71.
15. Altuntas, E.; Cayli G.; Kusefoglu, S; Nugay, N. *Designed Monom. Polym.* **2008**, *11*, 371.
16. Miyagawa, H.; Mohanty, A.; Drzal, L. T.; Misra, M. *Ind. Eng. Chem. Res.* **2004**, *43*, 7001.
17. Uyama, H.; Kuwabara, M.; Tsujimoto, T.; Nakano, M.; Usuki, A.; Kobayashi, S. *Macromol. Biosci.* **2004**, *4*, 354.
18. Song, B.; Chen, W.; Liu, Z.; Erhan, S. *Int. J. Plasticity* **2006**, *22*, 1549.
19. Haq, M.; Burgueno, R.; Mohanty, A. K.; Misra, M. *Compos. Sci. Technol.* **2008**, *68*, 3344.
20. Liu, Z. S.; Erhan, S. Z.; Xu, J. Y. *Polymer* **2005**, *46*, 10119.
21. Laus, M.; Camerani, M.; Lelli, M.; Sparnacci, K.; Sandrolini, F.; Francescangeli, D. *J. Mater. Sci.***1998**, *33*, 2883.
22. Zhu, J.; Morgan, A. B.; Lamelas, F. L.; Wilkie, C. A. *Chem. Mater.* **2001**, *13*, 3774.
23. Sen, S.; Memesa, M.; Nugay, N.; Nugay, T. *Polym. Int.* **2006**, *55*, 216.
24. Helvacioglu, E.; Aydin, V.; Nugay, T.; Nugay, N.; Uluocak, B. G.; Sen, S. *J. Polym. Res.* **2011**, *18*, 2341.
25. Lu, Y.; Larock, R. C. *Biomacromolecules* **2006**, *7*, 2692.
26. Sen, S.; Cayli G. *Polym. Int.* **2010**, *59*, 1122.
27. Cayli, G.; Kusefoglu, S. *Fuel Process. Technol.* **2008**, *89*, 118.
28. Cayli, G.; Kusefoglu, S. *J. Appl. Polym. Sci.* **2008**, *109*, 2948.
29. Koo, C. M.; Ham, H. T.; Choi, M. H.; Kim, S. O.; Chung, I. J. *Polymer* **2003**, *44*, 681.
30. Gilman, J. W. *Appl. Clay Sci.* **1999**, *15*, 31.
31. Dong, Z.; Wei, H.; Mao, J.; Wang, D., Yang, M.; Bo, S.; Ji, X. *Polymer* **2012**, *53*, 2074.
32. Bomfim, J. A. S.; Mincheva, R.; Beigbeder, A.; Persenaire, O.; Dubois, P. *e-polymers* **2009**, no. 035.
33. Lee, J.; Takekoshi, T.; Giannelis, E. *Mater. Res. Soc. Symp. Proc.* **1997**, *457*, 513.
34. Sen, S.; Nugay, N.; Nugay, T. *Polym. Int.* **2006**, *55*, 552.
35. Leszczynska, A.; Njuguna, J.; Pielichowski, K.; Banerjee, J. K. *Thermochim. Acta* **2007**, *453*, 75.
36. Kim, H. G.; Oh, D. H.; Lee, H. B.; Min, K. E. *J. Appl. Polym. Sci.* **2004**, *92*, 238.
37. Paris, R.; De la Fuente, J. L. *React. Funct. Polym.* **2007**, *67*, 264.
38. Venkatesh, R.; Vergouwen, F.; Klumperman, B. *J. Polym. Sci. Part A: Polym. Chem.* **2004**, *42*, 3271.
39. Noh, M. W.; Lee, D. C. *Polym. Bull.* **1999**, *42*, 619.
40. Landry, C. J. T.; Coltrain, B. K.; Landry, M. R. *Macromolecules* **1993**, *26*, 3702.